

Al/SiCp Functionally Graded Metal-matrix Composites Produced by Centrifugal Casting: Effect of Particle Grain Size on Reinforcement Distribution

A. Velhinho ^{(*) 1, 2}, P.D. Sequeira ³,

F. Braz Fernandes ^{1, 2}, J.D. Botas ², L.A. Rocha ^{3, 4}

¹ CENIMAT - Centro de Investigação em Materiais, Universidade Nova de Lisboa, Faculdade de Ciências e Tecnologia, Quinta da Torre, 2829-516 Caparica – PORTUGAL

² DCM - Departamento de Ciência dos Materiais, Universidade Nova de Lisboa, Faculdade de Ciências e Tecnologia, Quinta da Torre, 2829-516 Caparica – PORTUGAL

³ CIICS – Centro de Investigação em Comportamento de Superfícies, Universidade do Minho, Campus de Gualtar, 4800-058 Guimarães PORTUGAL

⁴ DEM –Departamento de Engenharia Mecânica, Universidade do Minho, Campus de Gualtar, 4800-058 Guimarães PORTUGAL

Keywords: Metal matrix composites, Functionally graded materials, Centrifugal casting, Quantitative image analysis.

Abstract. Functionally graded materials (FGM's), particularly in the form of Al-Si metal matrix composites (MMC's) selectively reinforced at the surface with SiC particles, are advanced materials, combining high wear resistance with high bulk toughness or even a thermal barrier at the surface. Centrifugal casting is one of the most effective methods for processing this type of MMC, but accurate control of the ceramic particles distribution/gradient in the metallic matrix has not yet been completely attained. In this work, precursor Al/SiC composites were prepared by rheocasting, using SiC particles and an Al-10Si-2.2 Mg alloy. Morphology of the SiC particles was previously characterized by laser interferometry and SEM. Differing grain sizes were selected as reinforcing elements. The MMC's were then molten and centrifugally cast in order to produce the FGM composites, whose structure and properties were investigated by XRD, quantitative image analysis of optical micrographs and longitudinal hardness profiles. Therefore, it was possible to evaluate the influence of the particle grain size on the structure and properties of the FGM. Apart from the evaluation of the effects of particle grain size *per se*, its influence when combined with differing casting conditions are reported as well.

Introduction

In order to achieve reproducible properties of Al metal matrix composites (MMC's), knowledge about the spatial distribution of the reinforcement is of significant, due to its implication in failure processes [1]. This concern becomes paramount in the case of ceramic particle reinforced functionally graded materials (FGM's).

Centrifugal casting is one of the most effective methods for processing SiC-particle reinforced Al-based FGM's [2-8]. However, complete understanding of the particle distribution and the mechanisms presiding over it has not yet been achieved. Several parameters have been identified with an influence in the FGM's characteristics, namely atmosphere in the neighbourhood of the melt, melt pouring temperature, mould temperature, thermal gradient across the mould, solidification rate, centrifugal force and pouring rate [2, 6, 7, 9, 10]. These parameters will influence several phenomena occurring when the liquid melt containing solid particles solidifies in the mould: interaction and/or chemical reactions between the solidification front and the moving particles; rate of variation of the

melt viscosity during solidification; interactions between particles and liquid; or the initial position of the particles in the mould, before starting their movement in the liquid [2; 11]. The balance between these phenomena will dictate the outcome in terms of particle distribution, overall microstructure and FGM properties.

The present work aims at extending the existing knowledge about the influence of material and operating parameters – namely particle size, coupled with the time to achieve the maximum acceleration conditions – on the structure and properties of FGM's.

Materials and Methods

Precursor conventional MMC's, with a reinforcement volume fraction of 0.1, were rheocast from privately produced Al–10Si–2.2Mg ingot material, which was reinforced by SiC particles. The chemical composition of the matrix alloy was controlled by optical emission spectroscopy, while a Coulter LS230 laser interferometer was used to determine size distribution of the SiC particles added to the melt. Measured median particle sizes (D_V) of SiC reinforcements were 12.3, 37.4 and 118.8 μm , respectively. Details of the rheocasting apparatus and technique pertain to previous works [8, 12-14].

Those MMC's were then re-molten and centrifugally cast under vacuum, using a Titancast 700 μP Vac induction furnace, to produce the FGM composites, in accordance with a procedure described in detail elsewhere [6-8]. In every case, when the molten MMC reached the desired pouring temperature, the centrifugation cycle, lasting for 90 s, was initiated, control being exerted over the time ($t_{\gamma\text{Max}}$) taken to reach the maximum acceleration* imposed on the material. Centrifugal force compels the molten to pass from its alumina crucible into a cylindrical graphite mould, where it cools down and solidifies. The FGM samples, cylindrical in shape, with 40 mm in both length and diameter, exhibit a longitudinal reinforcement distribution gradient. The processing conditions for the centrifugally cast FGM composite can be found in Table 1.

TABLE 1 – Processing conditions for the FGM's; the overall SiC_p volume fraction was 10 vol. % in every case, although three different SiC particle sizes were tested.

Condition set	D_V [μm]	$t_{\gamma\text{Max}}$ [s]	T_p [$^{\circ}\text{C}$]
A	12.3	5	850
B	12.3	17	850
I	37.4	5	850
J	37.4	17	850
K	118.8	5	850
L	118.8	17	850

For the evaluation of the material properties and corresponding reinforcement distribution, the samples were longitudinally sectioned and polished. Vickers hardness measurements were performed following a regular pattern, allowing the establishment of longitudinal and transversal hardness profiles, as well as hardness maps. Quantitative images analysis of the microstructure of the material was also performed in a regular pattern consisting of successive transversal alignments along the longitudinal section of the sample. In order to assure a statistically representative number of particles in each micrograph, different

magnifications were used: 200 x for $D_V = 12.3 \mu\text{m}$, 100 x for $D_V = 37.4 \mu\text{m}$ and 50 x for $D_V = 118.8 \mu\text{m}$. Measured parameters were the particle area fraction, f_A , and mean particle diameter, d_A .

Chosen samples were subjected to XRD peak intensity measurements for the SiC peak (0 0 75), using $\text{Cu}_{K\alpha}$ radiation, along the median lines in the longitudinal direction, in order to further characterize the SiC distribution.

Results and Discussion

* The maximum acceleration value is constant ($240.4 \text{ m}\cdot\text{s}^{-2}$; 24.5 g), being imposed by the furnace construction details. That value may, however, be attained within a variable delay $t_{\gamma\text{Max}}$.

Fig. 1 presents the longitudinal hardness profiles determined for the various condition sets experimented with. Generally speaking, increases in particle size are accompanied by higher hardness levels attained throughout the FGM samples. In addition, for $t_{\gamma\text{Max}} = 5$ s, the gradients generated by larger reinforcement particles are steeper and exhibit the maximum level near the surface, instead of at some distance below the surface [6,7]. The same happens under $t_{\gamma\text{Max}} = 17$ s for particle sizes 12.3 and 37.4 μm , but not for 118.8 μm . Independently of the casting conditions, these larger particles show a substantially different behaviour, since samples so reinforced present a very steep gradient, varying from very high hardness values in near-surface regions down to values which are near the un-reinforced matrix hardness, suggesting that a great majority of the particles concentrate near the surface, leaving other regions severely depleted.

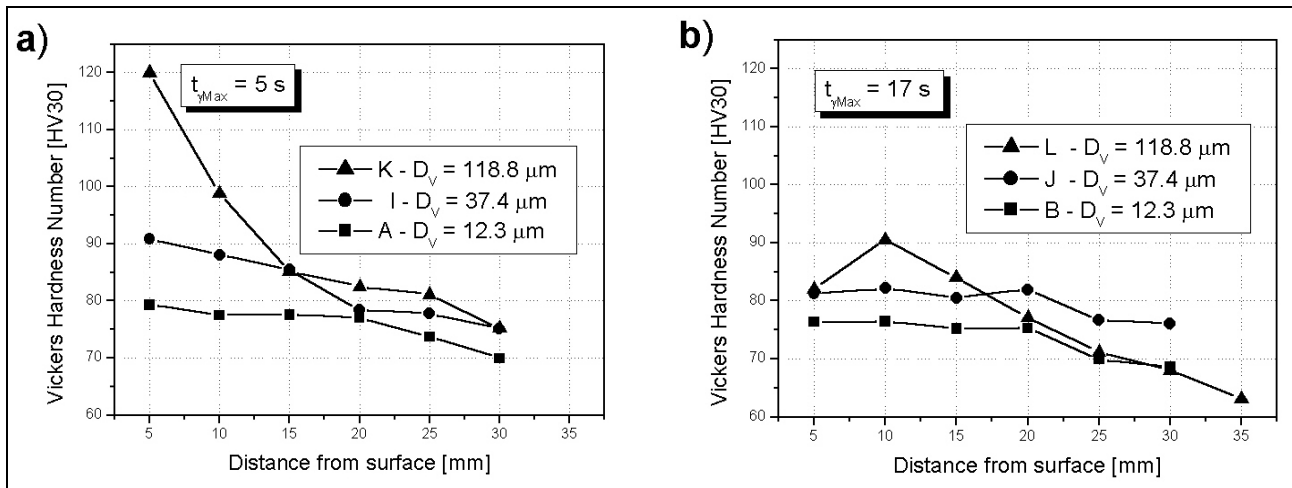


Figure 1 - Vickers hardness longitudinal profiles for FGM's reinforced with SiC particles of different median diameters. a) Vigorous casting conditions ($t_{\gamma\text{Max}} = 5$ s); moderate casting conditions ($t_{\gamma\text{Max}} = 17$ s).

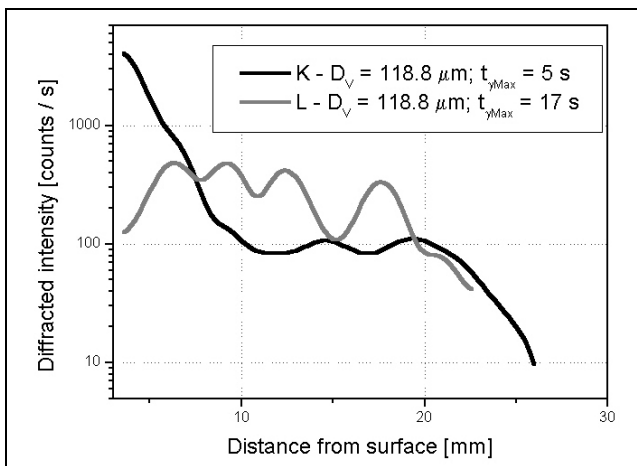


Figure 2 – XRD results showing the diffracted intensity from the SiC peak (0 0 75), as recorded along the FGM's median longitudinal line.

In Fig. 2 results of XRD SiC peak intensity measurements along the longitudinal direction are plotted. As it can be observed, the technique seems to provide reliable results when steep particle gradients are present (set K Fig. 1 a) and Fig. 2). However, when smooth gradients are present, noise originated by fluctuations in diffracted intensity caused by local variations in matrix grain size and SiC particle size becomes significant, inhibiting a correct assessment of the gradient (set L Fig. 1b) and Fig. 2).

Measurements of f_A obtained through quantitative image analysis are presented in Fig. 3, the results being in good general agreement with those from Fig. 1. For $t_{\gamma\text{Max}} = 5$ s, the samples reinforced with 12.3 or 37.4 μm particles present a very shallow gradient, coupled with just a slight superficial decrease in particle content relative to the maximum, which occurs around 5 mm below the surface. As to those reinforced with the larger particles, no peak occurs, and the particle content continuously decays from the surface to the interior, defining a steep gradient and revealing that at 12 mm below the surface the material is almost entirely devoid of reinforcements. When $t_{\gamma\text{Max}} = 17$ s,

one observes a similar behaviour for $D_V = 12.3$ and $37.4 \mu\text{m}$, albeit with more pronounced peaks; for $D_V = 118.8 \mu\text{m}$ there is a significant increase in f_A from the surface to the interior, with a subsequent less marked decrease. The existence of a depleted region ca 20-25 mm from the surface could be confirmed through conventional optical microscopy observations.

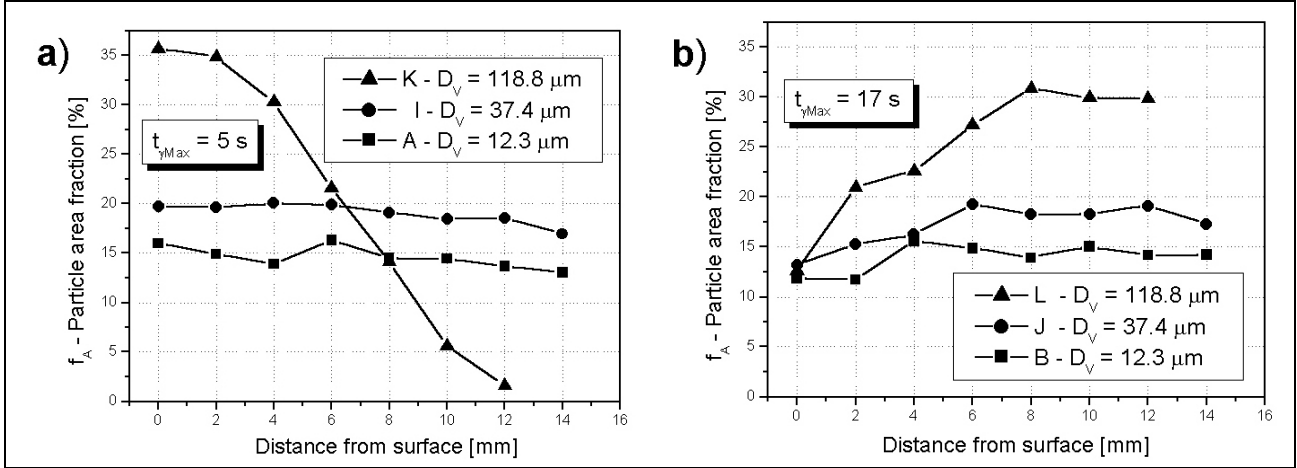


Figure 3 – Particle area fraction longitudinal profiles measured by quantitative image analysis of optical micrographs. a) Vigorous casting conditions ($t_{\gamma\text{Max}} = 5 \text{ s}$); moderate casting conditions ($t_{\gamma\text{Max}} = 17 \text{ s}$).

In Fig. 4 further measurements obtained through quantitative image analysis are presented, this time regarding the SiC particle size evolution along the samples. Except for condition K ($D_V = 118.8 \mu\text{m}$; $t_{\gamma\text{Max}} = 5 \text{ s}$), when the largest particles are the ones that attain the surface, in all other cases there is peak in d_A occurring at some distance from the surface. Furthermore, increases in $t_{\gamma\text{Max}}$ lead to decreased mean particle diameters at or near the surface. An exception exists regarding samples reinforced with $D_V = 12.3 \mu\text{m}$, in which an increase in mean particle diameter near the surface is obtained when less drastic casting conditions are used.

Discussion of the above-reported phenomena must take into account the Stoke's law [15]. According to this, the velocity (v) of a single spherical particle with a given diameter (D_p) and density (ρ_p) moving under constant acceleration (γ) across a fluid with a distinct density (ρ_l) and known viscosity (η), is given by:

$$v = \frac{D_p^2 (\rho_p - \rho_l) \gamma}{18 \eta} \quad (1)$$

This makes clear that, when under the effect of centrifugal force γ , particle segregation towards the surface of the cast is in first place due to the difference in density between the ceramic particles and the molten alloy ($\rho_{\text{SiC}} = 3.2 \text{ g cm}^{-3}$ vs. $\rho_{\text{Al alloy}} \sim 2.3 - 2.7 \text{ g cm}^{-3}$) [11]. Equation (1) also reveals the strong influence of the particle diameter: larger particles will be animated with higher velocities, in proportion to the square of the particle diameter. When a population of particles is present, if one does not consider particle interaction phenomena, it can be concluded that if the particle population is mainly composed of large particles (as is the case of $D_V = 118.8 \mu\text{m}$), particles will tend to attain higher velocities, i.e. to travel further, resulting in higher particle volume fractions near the surface when compared with the situation in which the population is composed of smaller particles. This effect is also likely to explain why a particle diameter gradient tends to appear within a given FGM sample, since the corresponding particle population naturally exhibits its own size distribution.

Yet further considerations are necessary in order to understand the reduction in particle area fraction and in mean particle diameter in regions near the surface, particularly for less severe casting

conditions.

Equation (1) also shows the influence of melt viscosity, from which stems a viscous drag force; this force, by opposing the particle movement, counteracts the effect of centrifugal acceleration. The melt viscosity involved is not simply the liquid intrinsic viscosity (η_l); given the presence of the ceramic particles, but also of an already solidified metallic fraction [2, 5, 6, 11], it will be an apparent viscosity (η_{app}) higher* than the value of η_l .

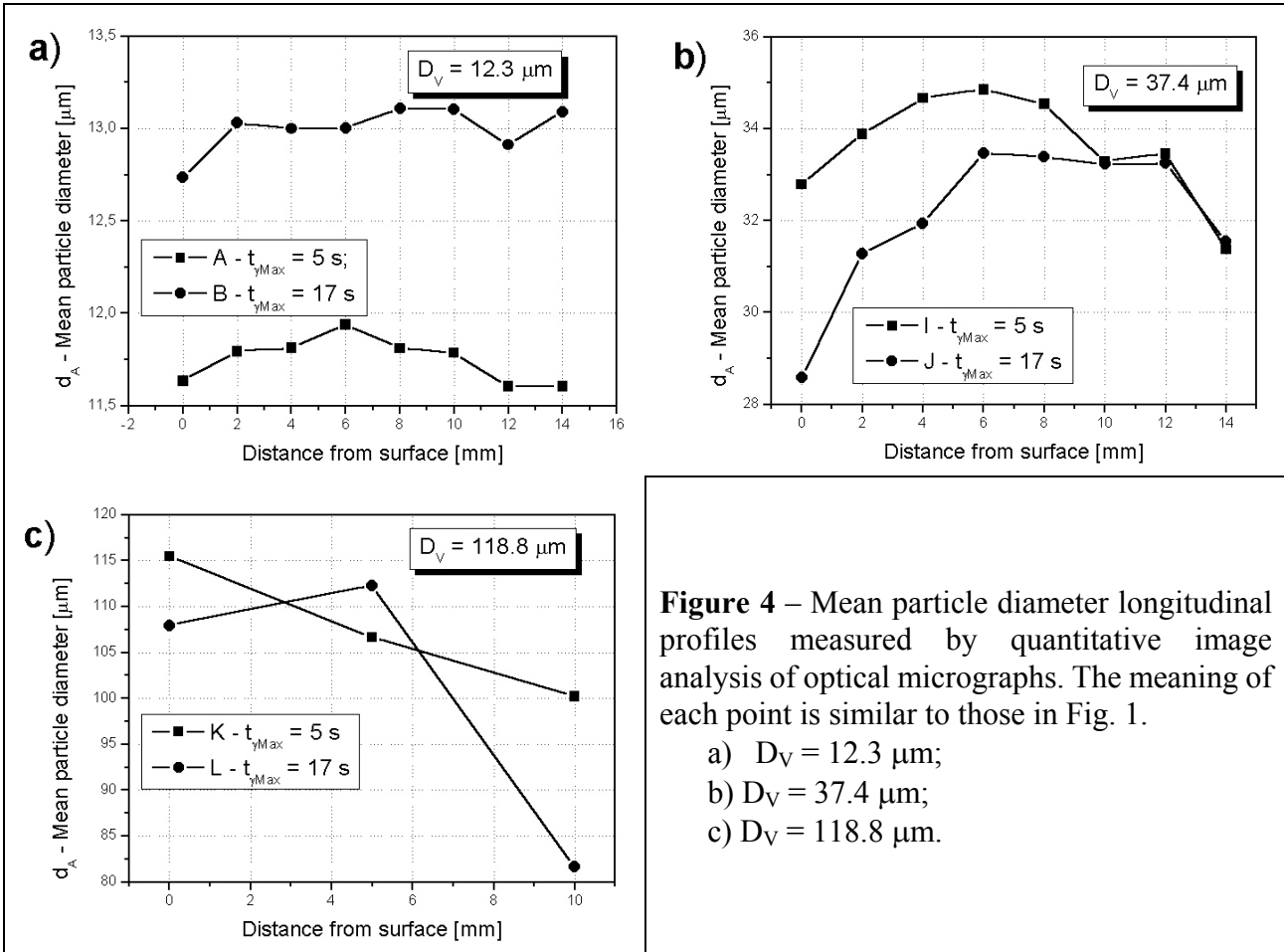


Figure 4 – Mean particle diameter longitudinal profiles measured by quantitative image analysis of optical micrographs. The meaning of each point is similar to those in Fig. 1.

- a) $D_v = 12.3 \mu\text{m}$;
- b) $D_v = 37.4 \mu\text{m}$;
- c) $D_v = 118.8 \mu\text{m}$.

Taking viscous drag, and its dependence from apparent viscosity of the melt, into account, it becomes understandable why in some conditions the amount of particles decreases near the surface, or why those particles reaching the surface are smaller. In fact, as SiC particles progress along the mould, during the casting operation, their increasing profusion progressively retards their travelling (due to mutual particle interactions), while at the same time the advance of the solidification front tends to impel those same particles towards the interior of the sample. The barrier effect from the advancing solidification front will be most effective for larger particles, since the remaining liquid channels may accommodate smaller ones while at the same time impeding the larger. Thus, if a large particle size is advantageous from the point of view of the attainable velocity imparted by centrifugal acceleration, this advantage can only be fully exploited when the maximum acceleration value is reached within a short delay, so that the particles reach the surface region before the advancing solidification front prevents them from doing so.

* Approximations abound to describe the dependency of η_{app} with the amount of particles (whether ceramic or metallic) suspended in the melt. See for instance Suresh and Mortensen [15], or Brinkman [16].

Conclusions

The effects of particle reinforcement grain size, coupled with variations in the delay to maximum centrifugal acceleration, on the properties and microstructure of centrifugally cast FGM Al/SiCp MMC's were studied. It was found that reinforcement with larger particles gives rise to higher hardness levels throughout the material, while at the same time originating steeper gradients than those obtained with smaller reinforcements. Particularly, if particles are large enough, total or partial particle depletion occurs in some regions away from the FGM surface.

Particle size near the surface decreases due to the effect of viscous drag caused by the advancing solidification front. However, this effect can be avoided by coupling large enough particle sizes, susceptible of attaining high terminal velocity, with short delays to reach the maximum centrifugal acceleration, which provide insufficient time for the development of a solidification-driven barrier to particle advance.

References

- [1] – T.W. Clyne, P.W. Withers, *An Introduction to Metal Matrix Composites*, (eds. E.A. Davis, I.M. Ward FRS, Cambridge University Press, United Kingdom 1993)
- (2) – Y. Watanabe, N. Yamanaka, Y. Fukui, *Composites Part A* Vol. 29A (1998) pp. 595-601
- (3) – Y. Watanabe, Y. Fukui, *Recent Res. Devel. Metallurg. & Materials Sci.*, Vol. 4 (2000) pp. 51-93
- (4) – Y. Watanabe, Y. Fukui, *Aluminum Transactions*, Vol. 2 (2000) 195-208
- (5) – Y. Watanabe, N. Yamanaka, Y. Oya-Seimira, Y. Fukui, *Zeitschrift fur Metallkunde*, Vol. 92 (2001) pp. 53-57
- (6) – L.A. Rocha, A.E. Dias, D. Soares, C.M. Sá, A.C. Ferro, *Ceramic Transactions*, Vol. 114 (2001) pp. 467-474
- (7) – L. A. Rocha, P. D. Sequeira, A. Velhinho, C. M. Sá, *Proc. XVI Congresso Brasileiro de Engenharia Mecânica* (Brasil 2001) pp. 381-388
- (8) – A. Velhinho, P.D. Sequeira, Rui Martins, G. Vignoles, F.M. Braz Fernandes, J.D. Botas, L.A. Rocha, *E-MRS Spring Meeting 2002* (France 2002); accepted for publication by Nuclear Instr. & Methods in Phys. B
- (9) – C.G. Kang, P.K. Rohatgi, *Met. & Mat. Trans. B* Vol. 27B (1996), pp. 277-285
- (10) – M. Mamoru, K.-I. Abe, T. and Inoue, J. of the *Jap. Soc. of Mat. Sci.* Vol. 46 (1997) pp. 946-951
- (11) – L. Lajoie, M. Suéry, *Proc. Int. Symp. on Advances in Cast Reinforced Metal Composites* (ASM International 1988), pp. 15-20
- (12) – C. Ferreira, J. Teixeira, J. D. Botas, *Proc. 8º Encontro da Soc. Portuguesa de Materiais* (Portugal 1997), pp. 9-18
- (13) – C. Ferreira, *Processos Tecnológicos Associados à Reo-Fundição* (PhD Thesis, Universidade Nova de Lisboa, Portugal 1999)
- (14) – A. Velhinho, F.M. Braz Fernandes, J.D. Botas, *Key Eng. Mat.* Vol. 230-232 (2002), pp. 226-230
- (15) – S. Suresh, A. Mortensen, *Fundamentals of Functionally Graded Materials: Processing and Thermomechanical Behaviour of Graded Metals and Metal-Ceramic Composites* (IOM Communications Ltd. 1998)
- (16) – H.C. Brinkman, *J. Chem. Phys.* Vol. 20 (1952) p. 571

Acknowledgements

Financial support by Fundação para a Ciência e Tecnologia (FCT - Portugal), under contract POCTI/12301/2001 and further support obtained by A. Velhinho from Fundo Social Europeu (program PRODEP), are gratefully acknowledged.